Magnetic polaron percolation on a rutile lattice: A geometrical exploration in the limit of low density of magnetic impurities

L. Sangaletti,[1] F. Federici Canova,[1] G. Drera,[1] G. Salvinelli,[1] M. C. Mozzati,[2] P. Galinetto,[2] A. Speghini,[3] and M. Bettinelli[4]

[1]*Dipartimento di Matematica e Fisica, Università Cattolica, via dei Musei 41, 25121 Brescia, Italy*

[2]*Dipartimento di Fisica A. Volta, Università di Pavia, 27100, Pavia, Italy*

[3]*DiSTeMeV, Università di Verona, via della Pieve 70, San Floriano, 37029 Verona, Italy*

[4]*Dipartimento Scientifico e Tecnologico, Università di Verona, Strada Le Grazie 15, 37134 Verona, Italy*

(Received 7 January 2009; revised manuscript received 21 April 2009; published 10 July 2009)

The evolution of magnetic polaron clusters on a rutile lattice has been explored, and the results are used to discuss the origin of ferromagnetism in transition-metal (TM)-doped rutile TiO_2 oxides. It is shown that percolation on a rutile lattice is characterized by a threshold different from that found for the percolation of randomly distributed spheres, which has been so far assumed as a model to treat the percolation of magnetic polarons in diluted magnetic semiconductors. Furthermore, unlike previous investigations, we explicitly considered the condition of small density n_i of TM impurities, i.e., a regime that is quite far from that usually regarded for polaron formation, dominated by a high density n_i of TM ions. Assuming that ferromagnetic coupling arises between polarons that share common TM impurities, we show the effect of this constraint on the magnetic properties of the sample compared to those reported for the $n_i \gg n_h$ regime.

DOI: 10.1103/PhysRevB.80.033201 PACS number(s): 75.50.Pp, 75.10.−b, 75.50.Dd

The evidence of room-temperature ferromagnetism (FM) reported for TiO_2-based oxides has triggered a large number of research activities aimed to identify the mechanism underlying ferromagnetic long-range order.[1–6] Among these studies, several models have been recently developed to account for the magnetization behavior as a function of temperature i.e., an M vs T curve that looks similar to those reported in paramagnetic systems. The intrinsically disordered distribution of magnetic cations in the lattice can be effectively treated with magnetic polaron models, as recently proposed for diluted magnetic semiconductors (DMSs) (Refs. 7–9) and then extended to the case of magnetism in diluted magnetic oxides (DMOs).[1] Following these studies, in the field of DMO the concepts of percolation and polarons have been recently applied to several cases, including the study of magnetic coupling in HfO_2 (Ref. 10) and the problem of electron transport in DMOs.[11]

Assuming the case of rutile TiO_2 as the host lattice, magnetic polaron model states that the localized holes created with an oxygen vacancy are described by a wave function such as

$$\psi(\vec{r}) = (\pi a_B^3)^{-1/2} e^{-r/a_B}, \tag{1}$$

where a_B is the localization radius of the hole. Due to the fact that these holes are diluted in the system, we can neglect direct exchange interaction between two nearby holes. This approximation can be extended to magnetic impurities as well. The sole magnetic interaction to consider is the direct exchange between a hole and a magnetic impurity. This interaction has been found to be antiferromagnetic for many systems. We further simplify the model approximating the hole to a hard sphere of radius r_p so we can state that magnetic impurities lying inside an hole sphere interact with the hole, aligning its spin antiparallel to the hole spin. All impurities outside the sphere do not interact. When two nearby holes share some impurities, both the holes will align their spins antiparallel to the impurities spin, thus forming a cluster. This way, it is possible to achieve long-range magnetic order combining short-range interactions between holes and impurities. The key feature of this mechanism is percolation. In order to measure a macroscopic magnetization, there has to be a percolating cluster, i.e., a cluster extended enough to touch all system boundaries. This means that the polaron radius at the critical temperature must be the system percolation threshold,

$$r_p(T_c) = R_{perc}. \tag{2}$$

This sets a constraint for r_p vs T determination discussed later.

The most exhaustive studies so far proposed have been focused on one specific regime, i.e., when the density n_i of magnetic impurities is greater than the density n_h of holes.[7,8] Due to the features of the magnetic polaron model, if $n_i > n_h$ it is highly probable that in any of the magnetic polarons a magnetic impurity can be found. This feature implies that polaron clusterization is basically a problem of spheres superposition, being the density n_i virtually constant in any of the cluster. However, there is an experimental evidence that ferromagnetism occurs also for $n_h \simeq n_i$,[12] a regime, that is largely unexplored. If the mechanism underlying the coupling of polarons is that determined by the presence of at least one magnetic impurity in the overlapping region, magnetic impurities have a relevant role not only to provide magnetic moment but also to determine the growth rate of the percolating cluster. This condition is particularly tight in the case of small density of magnetic impurities.

In this study we present the results of magnetic polaron percolation in DMO obtained from computational simulations carried out on a rutile lattice, in the regime of low density of transition-metal (TM) ions, and we compare the results with recent experimental data obtained from TiO_2 rutile single crystals.[12]

One of the major issues in developing a polaron model for

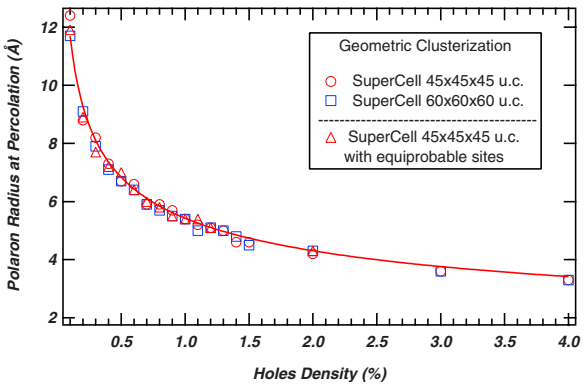

FIG. 1. (Color online) Percolation radius dependence on hole density. Simulations were carried out using a supercell with a 45 u.c. edge where the apical sites are more likely occupied by oxygen vacancies (circles) and where vacancies are equally distributed among all sites (triangles). Squares refer to data obtained using a supercell with 60 u.c. edge where the apical sites are more likely occupied by oxygen vacancies. In all cases, the geometric clusterization algorithm was used.

magnetization is to translate the r_p-dependent results into temperature-dependent results. Durst *et al.*[13] analyzed this problem and developed a T-dependent model to describe the dependence of r_p on T. In the literature, temperature effects are usually included on the basis of the equation,

$$r_p^3 n_h = \left[0.86 - (a_B^3 n_h)^{1/3} \ln \frac{T_c}{T} \right]^3, \tag{3}$$

that establishes a relation between the polaron radius and the temperature. This equation is a good interpolation for low temperatures of the simulated r_p vs T curve obtained by Durst *et al.*[13] In turn, for temperatures closer to T_c, the increase in r_p as the temperature is lowered is much slower. In the present calculations, we have transformed the results obtained as a function of r_p into temperature dependent results by considering the full range of the r_p vs T curve obtained by Durst *et al.*[13] Incidentally we observe that in Eq. (3), 0.86 that is the $r_p^3 n_h$ value at the percolation threshold for randomly distributed spheres is not suitable to treat the case of percolation in a rutile lattice, where $r_p^3 n_h$ resulted to be 0.467 from our simulations.

In Fig. 1, R_{perc} dependence on holes density n_h is shown, assuming that the polarons clusterize through simple superposition (hereafter denoted as geometric clusterization). We ran several simulations on supercells with different size and changed the holes population pattern. From these data we can see that a supercell with a 45 unit cell (u.c.) edge is large enough to provide statistically good results. It should be noted that changing the hole's population pattern does not induce a visible effect. Data obtained when oxygen vacancies are not equally distributed between apical and basal sites in the TiO_6 coordination octahedron are not different from those obtained by assuming an equiprobable distribution. Figure 1 shows the results obtained from a distribution where apical sites are 80% probable (against 20% for O basal sites). Interpolating the R_{perc} vs n_h data gives a law for percolation radius,

$$R_{perc} = \sqrt[3]{\frac{a}{n_h}}, \tag{4}$$

where $a=0.102 \pm 0.005$ is an adimensional parameter calculated by fitting data, which depends solely on the lattice structure. This equation is obtained from Eq. (3) by setting $T=T_c$ and substituting the value 0.86 with the proper value (i.e., $a^{1/3}=0.467$) for the crystal structure under consideration.

We ran simulations on a $45 \times 45 \times 45$ u.c. supercell introducing the impurities dependence in the clusterization algorithm, obtaining data shown in Fig. 2, top panel. Here R_{perc} dependence on n_h for some fixed values of n_i is shown. Assuming that the percolation radius depends on n_h as stated in Eq. (4) and that it depends on n_i in a similar way, we can fit data using the relation

$$R_{perc} = \sqrt[3]{\frac{a}{n_h}} + \sqrt[3]{\frac{b}{n_i}}, \tag{5}$$

where $b=0.5$ is a dimensionless parameter that depends on the lattice shape and is calculated from data interpolation. The R_{perc} dependence on n_i for some fixed n_h values is shown in Fig. 2, bottom panel.

We can directly count how many holes and impurities belong to the most extended cluster inside the supercell so it is possible to calculate the magnetization of the system. For the simulation we used a supercell populated with $n_h=1.5\%$ and $n_i=0.5\%$: the number of holes and impurities inside the largest cluster as function of polaron radius r_p is shown in Fig. 3 (top panel) for both clusterization methods. Excluding the role of impurities in the clusterization method leads to a fast hole aggregation at a relatively low r_p, while impurities join to the cluster more slowly. On the other side, clusterizing polarons with common impurities lead to an opposite situation, where the percolation threshold is higher; impurities (now needed to form a cluster) are suddenly included inside the cluster while holes join to it more slowly. When the density of impurities is increased (Fig. 3, bottom panel), their contribution to the largest cluster is clearly increased and, for $n_h=1.5\%$ and $n_i=4.0\%$, it is prevailing in the impurity clusterization for all polaron radius while it becomes dominant in the geometric clusterization scheme for $R_p \geq 7$.

Finally we discuss the magnetization of a system characterized by magnetic polaron percolation on a rutile lattice. According to the model proposed by Das Sarma,[7] one can obtain the system magnetization as follows:

$$M = S_i n_i P_\infty, \tag{6}$$

where S_i is the impurity magnetic momentum, n_i is the impurities density, and P_∞ is the volume of the biggest cluster in the system. This relation, which has been developed for what we defined the geometric percolation case, assumes that only the impurities give a relevant contribution to the total magnetization since they are far more than the holes so that they can be approximated to a uniform background. With our model we explored a different regime, where it is not possible to neglect the contribution arising from holes; anyway

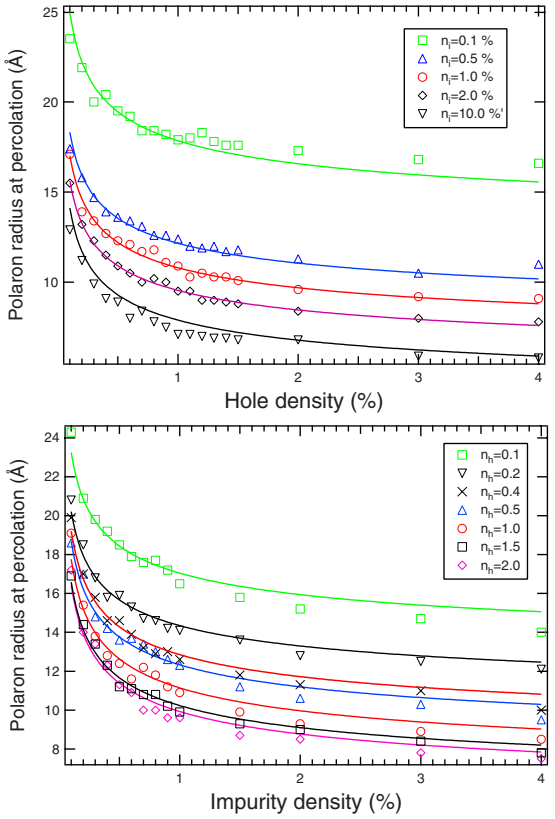

FIG. 2. (Color online) Top panel: percolation radius dependence on hole density obtained using a supercell with 45 u.c. edges. Different symbols represent data obtained with different fixed impurities density. Bottom panel: percolation radius dependence on impurities density obtained using a supercell with 45 u.c. edges. Different symbols represent data obtained with different fixed holes density. The algorithm clusterizes polarons with common impurities.

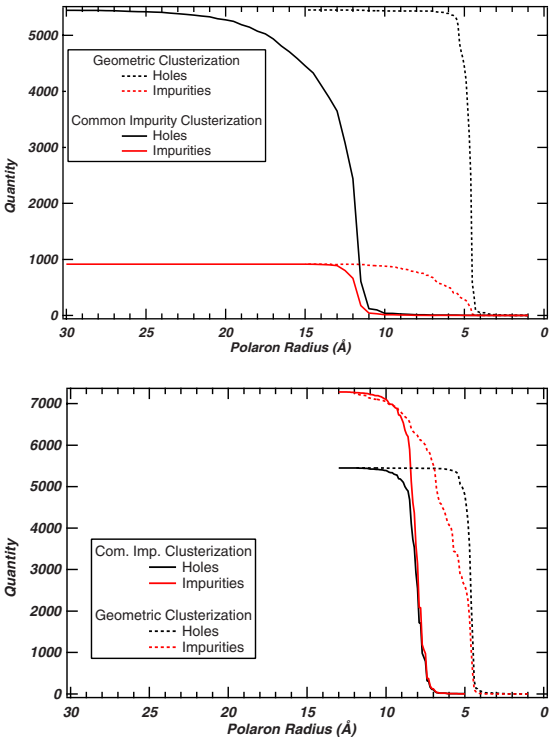

FIG. 3. (Color online) Top panel: holes (black line) and impurities (red line) amount in the largest cluster in a supercell with 45 u.c. edges. The system was populated with 1.5% holes and 0.5% impurities. Dashed lines refer to data calculated using the geometrical superposition, while solid lines refer to data obtained using the common impurity method. Bottom panel: same as above, with 1.5% holes and 4.0% impurities.

we can count the number of holes and impurities inside the biggest cluster as shown in Fig. 3 and it is possible to calculate the magnetization of the system as

$$M = |S_h N_h^{P_\infty} - S_i N_i^{P_\infty}| \tag{7}$$

where S_h and S_i are the hole and impurity magnetic moments and $N_h^{P_\infty}$ and $N_i^{P_\infty}$ are the total amount of holes and impurities inside the biggest cluster. This formula can be regarded as an extension of Eq. (6) as it also accounts for the hole magnetic moment. Since it is assumed that the spins of holes and impurities are antiparallel to each other,[13] we have to calculate the difference between the two contributions. We take the absolute value of this difference because an external magnetic field would align to its direction the greater of the two contributions. Using Eq. (7) we obtain the M vs T curves shown in Fig. 4, where the calculated data are plotted by assuming different n_i/n_h ratios. As can be observed, the overall behavior of the M vs T curve reproduces that experimentally observed for Co-doped rutile TiO_2 single crystals (inset of Fig. 4, adapted from Ref. 12) characterized by a low density of TM impurities.[14] The concave shape of the M vs T curve is typical of other similar systems[15] based on a rutile TiO_2 host lattice. For the TM ion a magnetic moment $S_i = 3/2$ is assumed, while $S_h = 1/2$ is related to each oxygen vacancy. The results are compared to those calculated for the geometric percolation scheme (dashed lines) by considering, through Eq. (6), only the contribution of $S_i = 3/2$ to the percolating cluster. Furthermore, it is clear that the concave shape of the curve is dependent on the concentration of TM impurities with respect to that of holes.

As for ferromagnetism in rutile, a recent theoretical study based on the LSDA+U approach[5] has shown that FM ordering can be found in Co-doped, oxygen substoichiometric, TiO_2 rutile through an interaction mediated by oxygen vacancies. However, in order to obtain a FM coupling, relatively high Co concentrations (12.5%) have been considered, which are far beyond the experimental cases we discuss in the present Brief Report. Furthermore, also a recent study on magnetism in HfO_2 (Ref. 10) has pointed out that in spite of the short-range FM ordering found up to the fourth nearest neighbor, the defect concentration required to place oxygen vacancies at this distance is not compatible with the observed physical properties of the system. In this respect, the polaron percolation model therefore seems to provide a possible explanation of FM ordering in very diluted systems. Only in the case of anatase TiO_2, a model based on superexchange interactions involving $[V_O^{2+}Co^{2+}]$ complexes (i.e., an oxygen vacancy and a magnetic impurity), has predicted ferromagnetic coupling already with 1% concentration of oxygen vacancies.[6] In this frame, the FM coupling is determined by

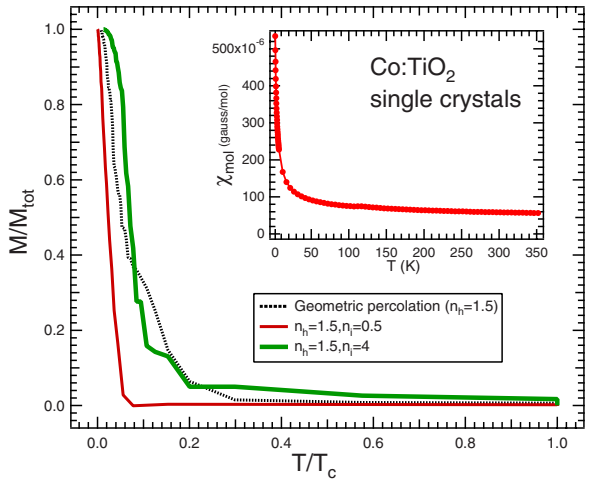

FIG. 4. (Color online) Calculated M vs T curves for samples with 1.5% holes and 0.5% impurities (red line) and 1.5% holes and 4.0% impurities (green line). The common impurity clusterization method is employed. For the TM ion a magnetic moment $S_i=3/2$ is assumed. The results are compared to those obtained for the geometric percolation scheme (dashed line) by considering only the contribution of $S_i=3/2$ to the percolating cluster. This curve has been computed on the basis of Eq. (6). In all three cases a_B was set at 1 Å. Inset: $CoTiO_2$ M vs T curve (adapted from Ref. 12).

superexchange between magnetic ions via empty levels generated by oxygen vacancies. Although this prediction has been obtained by partially referring to information available for oxygen-deficient rutile, being that information of the vacancy-related states in anatase TiO_2 is rather scanty, the approach of Kikoin and Fleurov[6] allowed estimation of the dependence of the Curie temperature on the chemical potential and should be regarded for future comparison with the predictions of the magnetic polaron model, especially in the case that the superexchange approach can be extended also to rutile-based systems.

Finally, we comment on the possibility to apply the magnetic polaron model to anatase. Actually, when the size of the polaron increases, the model seems to become quite insensitive to the crystal structure, e.g., to the site where either the magnetic impurity or the oxygen vacancy is placed (see, e.g., the discussion of Fig. 1 on the occupation of apical and basal sites by holes). Therefore, the magnetic polaron model could be applied to anatase as well, but the main difference with respect to rutile is represented by the localization radius a_B of the hole [Eq. (1)]. This radius is found to remarkably depend on several physical parameters, such as the dielectric constant and the effective mass. According to a recent study,[16] we have assumed for our calculation that $a_B=1.31$ nm in rutile, while for anatase a radius $a_B=0.48$ nm must be considered. On this basis, the growth rate of the magnetic polaron radius with temperature, and therefore the M vs T behavior, is determined by the size of a_B. Hence, the results of rutile could be extended to the case of anatase provided that the proper a_B value is accounted for. This represents a rather interesting perspective since several papers have been reported[17–20] on anatase samples that displayed a strongly dielectric behavior as the rutile single crystals mentioned in the present study.[12] For their vanishingly small free-carrier concentration, they have been proposed to be called dilute magnetic dielectrics. Also for these anatase samples, one has to account for a magnetic ordering that arises in a regime where both the impurity and oxygen vacancies concentration are very low, i.e., where the magnetic polaron model can be consistently applied. Incidentally, for some of the above-mentioned TiO_2 anatase samples,[17,18] the M vs T curve resembles that observed for the rutile single crystals that we are considering.

In conclusion, the percolation of magnetic polarons on a rutile lattice has been studied in large supercells, representative of bulk rutile TiO_2. We explicitly considered the condition of small density n_i of TM impurities, i.e., a regime that is quite far from that usually regarded for magnetic polaron formation, dominated by a high density n_i of TM ions. Assuming that ferromagnetic coupling arises between polarons that share common TM impurities, we showed the effect of this constraint on the magnetic properties of the sample compared to those reported for the $n_i \gg n_h$ regime. A proper formula for the calculation of magnetization in the common impurity approach has been proposed. The possibility of applying this model to the anatase phase is finally evaluated, showing that the model could be applied to anatase provided that the proper a_B radius is considered.

Financial support from the Cariplo foundation is acknowledged.

[1] J. M. Coey *et al.*, Nature Mater. **4**, 173 (2005).
[2] G. Mallia *et al.*, Phys. Rev. B **75**, 165201 (2007).
[3] J. Chen *et al.*, Phys. Rev. B **74**, 235207 (2006).
[4] L. A. Errico *et al.*, Phys. Rev. B **72**, 184425 (2005).
[5] V. I. Anisimov *et al.*, J. Phys.: Condens. Matter **18**, 1695 (2006).
[6] K. Kikoin *et al.*, Phys. Rev. B **74**, 174407 (2006).
[7] S. DasSarma *et al.*, Phys. Rev. B **67**, 155201 (2003).
[8] A. Kaminski *et al.*, Phys. Rev. Lett. **88**, 247202 (2002).
[9] M. J. Calderón *et al.*, Phys. Rev. B **75**, 235203 (2007).
[10] J. Osorio-Guillén *et al.*, Phys. Rev. B **75**, 184421 (2007).
[11] H. Chou *et al.*, Phys. Rev. B **77**, 245210 (2008).
[12] L. Sangaletti *et al.*, J. Phys.: Condens. Matter **18**, 7643 (2006).
[13] A. C. Durst *et al.*, Phys. Rev. B **65**, 235205 (2002).
[14] For these crystals a Co^{2+} molar concentration of about 0.1% was estimated from the paramagnetic contribution to the M vs H magnetization curve. Likewise, a concentration of about 0.4% of vacancies was estimated from the analysis of the undoped rutile single crystal.
[15] K. J. Kim *et al.*, J. Magn. Magn. Mater. **316**, e215 (2007).
[16] J. M. D. Coey, in *Local-Moment Ferromagnets*, Lecture Notes in Physics Vol. 678 (Springer, Berlin/Heidelberg, 2005), p. 185.
[17] K. A. Griffin *et al.*, J. Appl. Phys. **97**, 10D320 (2005).
[18] K. A. Griffin *et al.*, Phys. Rev. Lett. **94**, 157204 (2005).
[19] T. C. Kaspar *et al.*, Phys. Rev. B **73**, 155327 (2006).
[20] S. A. Chambers *et al.*, Appl. Phys. Lett. **79**, 3467 (2001).